

# Mouse Sperm Lacking Cell Surface Hyaluronidase PH-20 Can Pass through the Layer of Cumulus Cells and Fertilize the Egg\*

Received for publication, May 10, 2002  
Published, JBC Papers in Press, June 13, 2002, DOI 10.1074/jbc.M204596200

Daichi Baba‡, Shin-ichi Kashiwabara‡, Arata Honda‡, Kazuo Yamagata§, Qing Wu‡, Masahito Ikawa§, Masaru Okabe§, and Tadashi Baba¶

From the ‡Institute of Applied Biochemistry, University of Tsukuba, Tsukuba Science City, Ibaraki 305-8572, Japan, and the §Genome Information Research Center, Osaka University, Yamadaoka 3-1, Suita, Osaka 565-0871, Japan

**The function of glycosylphosphatidylinositol-anchored sperm hyaluronidase PH-20 in fertilization has long been believed to enable acrosome-intact sperm to pass through the layer of cumulus cells and reach the egg zona pellucida. In this study, we have produced mice carrying a null mutation in the PH-20 gene using homologous recombination. Despite the absence of sperm PH-20, the mutant male mice were still fertile. *In vitro* fertilization assays showed that mouse sperm lacking PH-20 possess a reduced ability to disperse cumulus cells from the cumulus mass, resulting in delayed fertilization solely at the early stages after insemination. Moreover, SDS-PAGE of sperm extracts and subsequent Western blot analysis revealed the presence of other hyaluronidase(s), except PH-20, presumably within the acrosome of mouse sperm. These data provide evidence that PH-20 is not essential for fertilization, at least in the mouse, suggesting that the other hyaluronidase(s) may play an important role in sperm penetration through the cumulus cell layer and/or the egg zona pellucida, possibly in cooperation with PH-20, although the importance of sperm motility cannot be neglected.**

Hyaluronic acid, a polymer consisting of repeating disaccharide units of *N*-acetyl-D-glucosamine and D-glucuronic acid, is one of the most common glycosaminoglycans present in the extracellular matrix of connective tissues (1–3). Because the structural and functional components in the extracellular matrix maintain the tissue architecture, hyaluronic acid is implicated in many physiological processes, including cell migration, proliferation, and differentiation. Hyaluronidase, which hydrolyzes hyaluronic acid to oligosaccharides, has been identified in mammalian, insect, and bacterial species (2, 3).

Fertilization in mammals requires sperm to pass through the layer consisting of the extracellular matrix of cumulus cells, and reach the egg zona pellucida (ZP)<sup>1</sup> (4–6). Because the

cumulus layer is abundant in hyaluronic acid (7), sperm have long been believed to possess a hyaluronidase activity that enables acrosome-intact sperm to penetrate the cumulus layer (4–6). A glycosylphosphatidylinositol-anchored membranous protein, PH-20, which was originally identified as a binding protein to the ZP in guinea pig sperm (8), is structurally similar to bee venom hyaluronidase and indeed exhibits hyaluronidase activity (9–13). When the enzyme activity of PH-20 is blocked, sperm are incapable of entering into the cumulus cell layer (14). The binding of acrosome-reacted sperm to ZP, known as “secondary sperm-ZP binding,” is also inhibited by antibody against PH-20 (15). Thus, these results imply that PH-20 is bifunctional. The N- and C-terminal domains of PH-20 have been reported to be responsible for hyaluronidase and ZP binding activities, respectively (15).

To explore the role of PH-20 *in vivo*, using homologous recombination we have produced male mice carrying a disruptive mutation in the PH-20 gene. The mice lacking PH-20 are still fertile, providing evidence that PH-20 is not essential for the penetration of sperm through the cumulus cell layer. Moreover, SDS-polyacrylamide gel electrophoresis (PAGE) in the presence of hyaluronic acid demonstrates the existence of other hyaluronidase(s) except PH-20 in mouse sperm. In particular, a hyaluronic acid-hydrolyzing protein with a size of ~55 kDa is abundantly present in soluble proteins released by A23187-induced acrosome reaction of sperm, including the acrosomal components. Thus, the process governing sperm penetration of the cumulus cell layer needs to be reassessed at least in the mouse model.

## EXPERIMENTAL PROCEDURES

**Generation of Mutant Mice Lacking PH-20**—Genomic clones encoding the PH-20 gene were isolated from a mouse 129/SvJ genomic DNA library in λFIXII (Stratagene) using a polymerase chain reaction (PCR)-amplified cDNA fragment as a probe. Of 10 clones isolated, two clones, termed mPHG3 and mPHG6, were used for construction of a targeting vector including a neomycin-resistance (*neo*) expression cassette flanked by a 1.5-kb genomic region of the PH-20 gene and an HSV-TK cassette (Fig. 1A). The construct was designed to replace a part of exon 2 with the *neo* expression cassette. Following electroporation of the targeting construct, which had been linearized by digestion with *Not*I, into mouse D3 embryonic stem (ES) cells, homologous recombinants were selected using G418 and gancyclovir as described previously (16). Five ES cell clones containing the targeted mutation were selected from 504 clones resistant to G418 and gancyclovir and injected into C57BL/6 mouse blastocysts. Chimeric male mice were crossed to C57BL/6 or ICR females (Japan SLC Inc., Shizuoka, Japan) to establish heterozygous mutant lines. Homozygous null mice were obtained by heterozygous mating.

**Blot Hybridization**—Genomic DNA was prepared from mouse tail, digested by *Bgl*II, separated by agarose gel electrophoresis, and transferred onto Hybond-N<sup>+</sup> nylon membranes (Amersham Biosciences). Total cellular RNA was also separated by agarose gel electrophoresis and transferred onto the nylon membranes. The blots were probed by <sup>32</sup>P-labeled DNA fragments and analyzed by a BAS-1800II Bio-Image analyzer (Fuji Photo Film, Tokyo) as described previously (17).

**Preparation of Antibody**—Recombinant mouse PH-20 produced in

\* This work was supported in part by grant-in-aids for scientific research on priority areas (B), scientific research (A), and exploratory research from the Japan Society for the Promotion of Science and the Ministry of Education, Culture, Sports, Science and Technology in Japan. The costs of publication of this article were defrayed in part by the payment of page charges. This article must therefore be hereby marked “advertisement” in accordance with 18 U.S.C. Section 1734 solely to indicate this fact.

¶ To whom correspondence should be addressed. Tel./Fax: 81-298-53-6599; E-mail: acroman@sakura.cc.tsukuba.ac.jp.

<sup>1</sup> The abbreviations used are: ZP, zona pellucida; HSV-TK, herpes simplex virus-thymidine kinase; ES, embryonic stem; PBS, phosphate-buffered saline; AI, proteins extracted from acrosome-intact sperm with *n*-octyl-β-D-glucopyranoside; AR, proteins extracted from acrosome-reacted sperm with *n*-octyl-β-D-glucopyranoside; SPA, soluble proteins released by A23187-induced acrosome reaction of sperm including acrosomal components; MPA, proteins on the plasma and outer acrosomal membranes fused during the acrosome reaction.

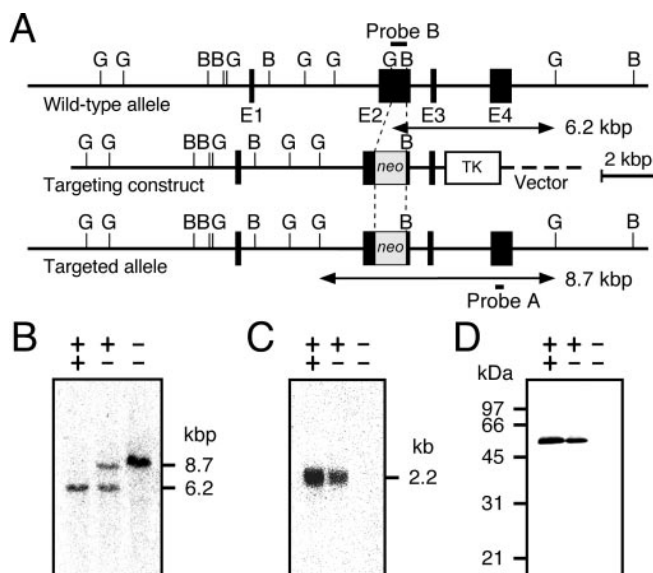


**FIG. 1. Generation of mice lacking PH-20.** A, targeting of the mouse *PH-20* gene. Restriction maps of the wild-type *PH-20* gene consisting of four exons (*E1–E4*, closed boxes), the targeting construct, and the predicted targeted gene are represented. A part of exon 2 (*E2*) encoding the hyaluronidase domain in the *PH-20* gene was replaced by a neomycin-resistance (*neo*) expression cassette (shaded boxes). The herpes simplex virus-thymidine kinase gene (*TK*, open box) was included in the targeting construct for negative selection using gancyclovir. Restriction enzyme sites indicated are as follows: *B*, *Bam*HI; *G*, *Bgl*II. B, Southern blot analysis of genomic DNA from wild-type (*Ph20*<sup>+/+</sup>, +/+), heterozygous (*Ph20*<sup>+/-</sup>, +/-), and homozygous (*Ph20*<sup>-/-</sup>, -/-) mice for the null mutation of the *PH-20* gene. Genomic DNA was prepared from the tail, digested by *Bgl*II, separated by agarose gel electrophoresis, and subjected to Southern blot analysis using a <sup>32</sup>P-labeled DNA fragment (*Probe A*, see panel A) as a probe. The wild-type and targeted alleles yielded 6.2- and 8.7-kbp DNA bands, respectively. C, Northern blot analysis of total cellular RNA from *Ph20*<sup>+/+</sup> (+/+), *Ph20*<sup>+/-</sup> (+/-), and *Ph20*<sup>-/-</sup> (-/-) mouse testes. The blots were probed by <sup>32</sup>P-labeled *Probe B*, as indicated in panel A. No mRNA signal of *PH-20* with a size of 2.2 kb was detected in the *Ph20*<sup>-/-</sup> mouse. D, Western blot analysis of sperm protein extracts from *Ph20*<sup>+/+</sup> (+/+), *Ph20*<sup>+/-</sup> (+/-), and *Ph20*<sup>-/-</sup> (-/-) mice. Proteins were extracted from cauda epididymal sperm with *n*-octyl- $\beta$ -D-glucopyranoside, separated by SDS-PAGE under nonreducing conditions, transferred onto polyvinylidene difluoride membranes, and probed by affinity-purified anti-mouse PH-20 antibody. The protein extracts of *Ph20*<sup>-/-</sup> mouse sperm did not contain an immunoreactive 52-kDa protein corresponding to PH-20.

insect cells was a kind gift from Dr. P. Primakoff (University of California at Davis). The recombinant protein (10  $\mu$ g) was emulsified by sonication in an equal volume of Freund's complete adjuvant (Difco Laboratories) and injected intradermally into female rabbits as described (18). Rabbit anti-mouse PH-20 antibody was purified by fractionation with ammonium sulfate (0 to 40% saturation) followed by immunoaffinity chromatography on columns of Sepharose 4B that had been conjugated with recombinant polypeptides produced in *Escherichia coli* containing 313 and 165 amino acids at residues 36–348 and 348–512 in the N- and C-terminal regions of mouse PH-20, respectively.

**Preparation of Protein Extracts**—Fresh cauda epididymal sperm were collected in a modified Krebs-Ringer bicarbonate solution (TYH medium) (19) containing 50 mM Hepes, washed with phosphate-buffered saline (PBS) by centrifugation at 800  $\times$  *g* for 10 min, and extracted in PBS containing 30 mM *n*-octyl- $\beta$ -D-glucopyranoside (Dojindo, Kumamoto, Japan), 1 mM EDTA, 1 mM benzamidine/HCl, 1 mM phenylmethanesulfonyl fluoride, leupeptin (1  $\mu$ g/ml), and pepstatin A (1  $\mu$ g/ml) at 4  $^{\circ}$ C for 6 h. The sperm suspension was centrifuged at 13,000  $\times$  *g* for 10 min. The supernatant solution was used as "sperm protein extracts."

**Measurement of Enzyme Activity**—Hyaluronidase activity was measured by the colorimetric method using Alcian Blue 8 GX (Sigma), as described previously (20). Briefly, the reaction was conducted in a mixture (0.6 ml) of 50 mM sodium acetate, pH 6.0, containing 50 mM MgCl<sub>2</sub>, 40  $\mu$ g of human umbilical cord hyaluronic acid (Sigma), and an appropriate amount of enzyme. Following incubation at 37  $^{\circ}$ C for 30 min, the reaction mixture was mixed with 0.02% Alcian blue solution

(0.6 ml), and centrifuged at 13,000  $\times$  *g* for 5 min. Absorbance of the supernatant solution at 603 nm was measured using a Shimadzu UV-160 spectrophotometer. A standard curve of hyaluronidase activity was obtained using bovine testicular hyaluronidase (295 units/mg, Sigma H3506) under the above described conditions.

**Fractionation of Sperm Proteins**—Cauda epididymal sperm in Hepes-buffered TYH medium (5  $\times$  10<sup>7</sup> sperm/ml) were induced to undergo acrosome reaction by the addition of calcium ionophore A23187 (Sigma) at a final concentration of 5  $\mu$ g/ml followed by incubation at 37  $^{\circ}$ C for 1 h under 5% CO<sub>2</sub> in air (21). The sperm suspension was centrifuged twice at 800  $\times$  *g* for 10 min to remove contaminating sperm. The supernatant was then centrifuged in a Beckman Optima MAX-E Ultracentrifuge using a TLA-100.3 rotor at 100,000  $\times$  *g* for 90 min. The resulting supernatant was used as a source of soluble proteins released by the A23187-induced acrosome reaction, including acrosomal components (SPA fraction). The precipitate obtained by ultracentrifugation was washed with PBS and extracted at 4  $^{\circ}$ C for 6 h in PBS containing 30 mM *n*-octyl- $\beta$ -D-glucopyranoside, 1 mM EDTA, 1 mM benzamidine/HCl, 1 mM phenylmethanesulfonyl fluoride, leupeptin (1  $\mu$ g/ml), and pepstatin A (1  $\mu$ g/ml), as described above. After centrifugation at 13,000  $\times$  *g* for 10 min, the supernatant was used as a source of membranous proteins on the plasma and outer acrosomal membranes fused during the acrosome reaction (MPA fraction). Proteins were also extracted from acrosome-intact and acrosome-reacted sperm with the same PBS containing *n*-octyl- $\beta$ -D-glucopyranoside and protease inhibitors (AI and AR fractions, respectively). The concentrations of proteins in the four fractions were determined using a Coomassie protein assay reagent kit (Pierce).

**SDS-PAGE and Western Blot Analysis**—Proteins were separated by SDS-PAGE under nonreducing conditions and transferred onto Immobilon-P polyvinylidene difluoride membranes (Millipore). After blocking with 2% skim milk, the blots were incubated with affinity-purified anti-mouse PH-20 antibody at room temperature for 2 h and then incubated with horseradish peroxidase-conjugated goat anti-rabbit IgG (Jackson Immunoresearch Laboratories) for 1 h. The immunoreactive proteins were detected by an ECL Western blotting detection kit (Amersham Biosciences). To detect proteins exhibiting hyaluronidase activity, SDS-PAGE in the presence of 0.01% human umbilical cord hyaluronic acid was carried out under nonreducing conditions as described previously (22). Following electrophoresis, gels were washed with 50 mM sodium acetate buffer, pH 6.0, containing 150 mM NaCl and 3% Triton X-100 at room temperature for 2 h to remove SDS and then incubated in the same buffer without Triton X-100 at 37  $^{\circ}$ C overnight. The hyaluronic acid-hydrolyzing proteins were visualized as transparent bands against a blue background by staining the gels with 0.5% Alcian Blue 8 GX and Coomassie Brilliant Blue R250 (Sigma).

**Fertilization Assays in Vitro**—Female ICR mice (8 weeks old) were superovulated by intraperitoneal injection of pregnant mare's serum gonadotropin (5 units) followed by human chorionic gonadotropin (5 units) 48 h later. Eggs were collected from the oviductal ampulla of the superovulated mice at 15–16 h after injection of human chorionic gonadotropin and placed in an 0.2-ml drop of TYH medium (19) covered with mineral oil. Fresh cauda epididymal sperm from ~3-month-old mice were capacitated by incubation for 2 h in a 0.2-ml drop of TYH medium at 37  $^{\circ}$ C under 5% CO<sub>2</sub> in air. An aliquot of the capacitated sperm suspension (1.5  $\times$  10<sup>5</sup> sperm/ml) was mixed with the eggs in TYH medium. The eggs and sperm were incubated for 0.5–6 h at 37  $^{\circ}$ C under 5% CO<sub>2</sub> in air. At the end of incubation, the eggs were briefly treated with bovine testicular hyaluronidase, fixed with glutaraldehyde, and then mounted on slides for whole-mount preparation. The eggs were stained with 0.25% lacmoid for the assessment of *in vitro* fertilization as described (16, 23).

For competitive fertilization assay *in vitro*, eggs with or without associated cumulus cells were incubated with an equally mixed suspension of wild-type and PH-20-deficient mouse sperm. The final concentrations of sperm were 1.5  $\times$  10<sup>5</sup> and 5.0  $\times$  10<sup>4</sup> sperm/ml for the cumulus-intact and cumulus-free eggs, respectively. Following incubation at 37  $^{\circ}$ C for 6 h, the fertilized eggs were washed twice with a modified simplex-optimized medium, kSOM/AA (24), and incubated at 37  $^{\circ}$ C for 96 h under 5% CO<sub>2</sub> in air. Each of the developing embryos was lysed in a 0.04% SDS solution (2  $\mu$ l) containing 24 mM NaOH by boiling for 3 min and was then used as a template for PCR amplification. The PCR reaction was carried out in a 40- $\mu$ l mixture containing 10 mM Tris-HCl, pH 8.8, 50 mM KCl, 1.5 mM MgCl<sub>2</sub>, 0.1% Triton X-100, dATP, dCTP, dGTP, and dTTP each at 0.2 mM, the oligonucleotide primers each at 1  $\mu$ M, template DNA, and 1 unit of Gene Taq DNA polymerase (Nippon Gene, Toyama, Japan), using MHA3 (5'-TTGAAGTCCAATC-GACAAGCT-3'), MHA16 (5'-GGTATTTCAGAGGTACGATCAG-3'), and

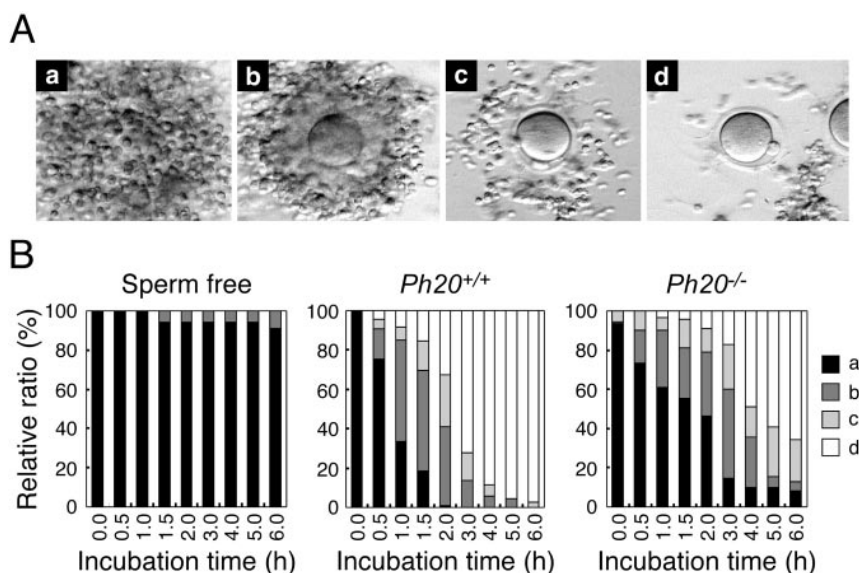


**FIG. 2. Dispersal of cumulus cells from the cumulus cell mass by mouse sperm lacking PH-20.** A, criterion of the status of the cumulus cell mass surrounding a mouse egg. The status of the cumulus mass after insemination *in vitro* was categorized as follows. If the eggs were tightly packed with cumulus cells, the status was defined as pattern *a* (the eggs were not observed clearly under a microscope). The pattern *b* eggs were loosely associated with the cumulus mass but still retained many cumulus cells. If most of the cumulus cells had been dispersed from the mass but the eggs still retained some cumulus cells, and if the eggs completely lost cumulus cells, the status was classified as patterns *c* and *d*, respectively. B, delayed dispersal of cumulus cells from the cumulus cell mass by mouse sperm lacking PH-20. The cumulus masses were inseminated by capacitated epididymal sperm of the wild-type (*Ph20*<sup>+/+</sup>) and PH-20-deficient (*Ph20*<sup>-/-</sup>) mice, and the status of the masses (closed, darkly shaded, lightly shaded, and open boxes for patterns *a*, *b*, *c*, and *d*, respectively) was assessed at time intervals indicated. Total numbers of 141 and 110 eggs were examined for *Ph20*<sup>+/+</sup> and *Ph20*<sup>-/-</sup> mouse sperm, respectively. The cumulus cell masses were also incubated in the absence of sperm as a control (*Sperm free*).

NP1 (5'-TCGTGCTTTACGGTATCGCCGGCTCCCGATT-3') as primers. The reaction program consisted of 35 cycles of 94 °C for 60 s, 60 °C for 60 s, and 72 °C for 30 s. The DNA products amplified were analyzed by PAGE as described previously (25).

## RESULTS

To elucidate the functional role(s) of PH-20 in fertilization, the mouse *PH-20* gene was disrupted in ES cells by homologous recombination using a targeting construct containing *neo* and *HSV-TK* expression cassettes (Fig. 1A). A part of exon 2 (E2) coding for the hyaluronidase domain in the *PH-20* gene was replaced by the *neo* cassette. Two of five independent ES cell clones carrying a mutated allele generated chimeric mice transmitting the allele to progeny. The genotypes of wild-type (*Ph20*<sup>+/+</sup>), heterozygous (*Ph20*<sup>+/-</sup>), and homozygous (*Ph20*<sup>-/-</sup>) mice for the null mutation of the *PH-20* gene were determined by Southern blot analysis of genomic DNA (Fig. 1B). Northern blot analysis of testicular RNA demonstrated the absence of *PH-20* mRNA in the *Ph20*<sup>-/-</sup> mouse (Fig. 1C). The level of the *PH-20* mRNA in the *Ph20*<sup>+/-</sup> mouse was ~50% of that in the wild-type mouse. Moreover, protein extracts of cauda epididymal sperm from *Ph20*<sup>-/-</sup> mice completely lacked an immunoreactive 52-kDa protein corresponding to PH-20 when affinity-purified anti-mouse PH-20 antibody was used as a probe (Fig. 1D). These data conclusively show the absence of PH-20 in *Ph20*<sup>-/-</sup> mouse sperm.

Male and female *Ph20*<sup>-/-</sup> mice were normal in behavior, body size, and health condition. Morphological analysis demonstrated no significant difference of the shapes, numbers, and sizes of testicular germ cells and epididymal sperm among *Ph20*<sup>+/+</sup>, *Ph20*<sup>+/-</sup>, and *Ph20*<sup>-/-</sup> mice (data not shown). Both the formation of copulation plugs in mated female mice and the motility of cauda epididymal sperm were also normal in the heterozygotes and homozygotes. Moreover, male *Ph20*<sup>-/-</sup> mice showed normal fertility and produced an average litter size (means ± S.E. = 13.8 ± 0.4, 13.6 ± 1.4, and 12.2 ± 0.8 for 5, 5, and 21 litters in *Ph20*<sup>+/+</sup>, *Ph20*<sup>+/-</sup>, and *Ph20*<sup>-/-</sup> mice, respec-

tively). Essentially similar results were obtained in the mouse lines derived from two independent ES clones. Therefore, these results provide evidence that PH-20 is not essential for fertilization at least in the mouse. Female *Ph20*<sup>-/-</sup> mice also exhibited normal fertility.

To examine whether the absence of PH-20 affects the process of sperm penetration through the layer of cumulus cells, *in vitro* fertilization analysis was carried out using capacitated cauda epididymal sperm. We have categorized the status of the mass of cumulus cells surrounding an egg into four patterns (patterns *a*, *b*, *c*, and *d*) to monitor successive dispersal of cumulus cells from the mass (Fig. 2A). When the cumulus cell mass was incubated in the absence of sperm, cumulus cells were spontaneously broken away from the mass. However, the eggs were still associated with many cumulus cells (patterns *a* and *b*) in the masses even after the incubation for 6 h (Fig. 2B). *Ph20*<sup>+/+</sup> mouse sperm readily dispersed cumulus cells from the mass, and ~70% of the eggs completely lost cumulus cells (pattern *d*) 3 h after insemination. As compared with the wild-type mouse, the *Ph20*<sup>-/-</sup> mouse showed a remarkable delay in the dispersal of cumulus cells from the mass. The ratio of the pattern *d* cumulus cell mass was less than 20% in the *Ph20*<sup>-/-</sup> mouse at 3 h after insemination. Thus, the delayed dispersal of cumulus cells may reflect the reduced ability of *Ph20*<sup>-/-</sup> mouse sperm to hydrolyze hyaluronic acid in the extracellular matrix of cumulus cells.

As shown in Fig. 3A, an *in vitro* fertilization assay confirmed the fertility of *Ph20*<sup>-/-</sup> mouse sperm. Although *Ph20*<sup>+/+</sup> and *Ph20*<sup>-/-</sup> mouse sperm equally fertilized the eggs 3 h after insemination, the rate of fertilization in *Ph20*<sup>-/-</sup> mouse sperm was significantly lower than that in *Ph20*<sup>+/+</sup> mouse sperm solely at the early stages (1 and 2 h) after insemination. To verify the delayed fertilization of *Ph20*<sup>-/-</sup> mouse sperm, eggs with or without associated cumulus cells were inseminated with an equally mixed suspension of *Ph20*<sup>+/+</sup> and *Ph20*<sup>-/-</sup> mouse sperm. The fertilized eggs with male and female pronu-

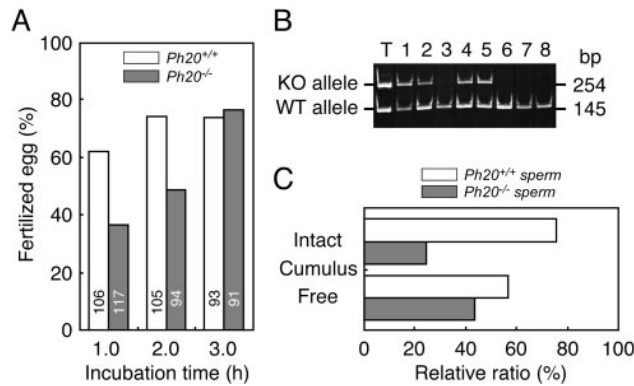


**FIG. 3. *In vitro* fertilization assay of mouse sperm lacking PH-20.** A, delayed fertilization of mouse sperm lacking PH-20 with cumulus-intact eggs. Cauda epididymal sperm of the wild-type ( $Ph20^{+/+}$ , open column) and PH-20-deficient ( $Ph20^{-/-}$ , shaded column) mice were capacitated and incubated with metaphase II-arrested, cumulus-intact eggs for 1, 2, or 3 h. After the incubation, the eggs were washed with TYH medium (see Ref. 19), treated briefly with bovine testicular hyaluronidase, washed, and then re-incubated for 5, 4, or 3 h (total incubation time = 6 h). The eggs with female and male pronuclei were defined as “fertilized eggs.” The numbers in the columns represent the numbers of eggs examined. B, PCR analysis of genomic DNA of the embryos developed from fertilized eggs *in vitro*. Metaphase II-arrested eggs with (235 eggs) or without associated cumulus cells (268 eggs) were incubated with an equally mixed suspension of  $Ph20^{+/+}$  and  $Ph20^{-/-}$  mouse sperm. After incubation for 6 h, the fertilized eggs were further incubated for 96 h. Genomic DNA was prepared from each of the developing embryos and then used as a template for PCR amplification. Two DNA fragments with the sizes of 254 and 145 bp, originated from the null-mutated (KO) and wild-type (WT) alleles, respectively, were detected by PAGE. The patterns of  $Ph20^{-/-}$  mouse tail (lane T) and eight developing embryos (lanes 1–8) are indicated. C, competitive fertilization assay of cauda epididymal sperm with cumulus-intact and cumulus-free eggs. Metaphase II-arrested eggs with or without associated cumulus cells were incubated with an equally mixed suspension of  $Ph20^{+/+}$  (open column) and  $Ph20^{-/-}$  (shaded column) mouse sperm, and the genotype of each of the developing embryos was assessed by PCR analysis as described in B above.

clei were then developed into embryos *in vitro*, and the genotype of each of the embryos was assessed by PCR. Two DNA fragments with the sizes of 254 and 145 nucleotides, which were PCR-amplified from the null-mutated and wild-type alleles, respectively, were detected (Fig. 3B). When the cumulus-intact eggs were used,  $Ph20^{-/-}$  mouse sperm were approximately three times slower to fertilize the eggs than  $Ph20^{+/+}$  mouse sperm (Fig. 3C). In the cumulus-free eggs, the fertilization rate in  $Ph20^{-/-}$  mouse sperm was still slow but close to that in  $Ph20^{+/+}$  mouse sperm. These data imply that the reduced fertilization rate in  $Ph20^{-/-}$  mouse sperm may be due to the delay of the sperm penetration through the cumulus cell layer.

Despite the time delay,  $Ph20^{-/-}$  mouse sperm are indeed capable of penetrating the layer of cumulus cells. This fact raises a possibility that other hyaluronidase(s) besides PH-20 may be present in mouse sperm and may participate in the sperm penetration through the cumulus layer, possibly in cooperation with PH-20. To ascertain this possibility, acrosome-intact sperm were extracted with *n*-octyl- $\beta$ -D-glucopyranoside, and total hyaluronidase activities in the sperm protein extracts were measured (Fig. 4A). The activities in the  $Ph20^{+/+}$  and  $Ph20^{-/-}$  mice were found to be ~80 and 40% of that in the  $Ph20^{+/+}$  mouse, respectively. SDS-PAGE in the presence of hyaluronic acid revealed that  $Ph20^{+/+}$ ,  $Ph20^{+/-}$ , and  $Ph20^{-/-}$  mouse sperm all contain a hyaluronic acid-hydrolyzing protein(s) with an approximate size of 55 kDa (Fig. 4B). A relatively sharp band of an enzymatically active 52-kDa protein was completely absent only in the  $Ph20^{-/-}$  mouse. Consequently, the 52-kDa protein corresponds to PH-20, which is

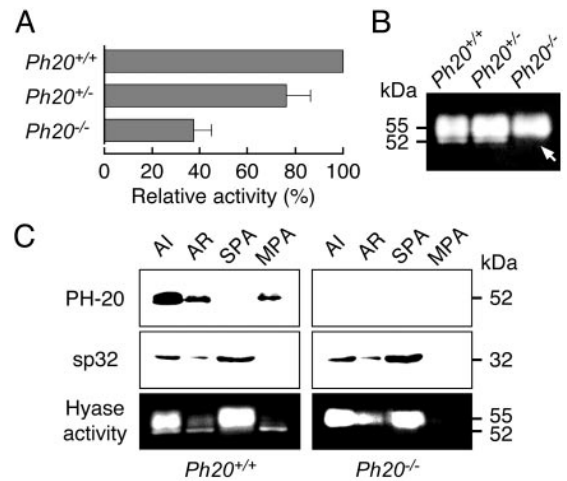


**FIG. 4. Presence of hyaluronidase(s) other than PH-20 in mouse sperm.** A, total hyaluronidase activity in sperm protein extracts. Acrosome-intact sperm from wild-type ( $Ph20^{+/+}$ ), heterozygous ( $Ph20^{+/-}$ ), and homozygous ( $Ph20^{-/-}$ ) mice for the null mutation of the PH-20 gene were extracted with *n*-octyl- $\beta$ -D-glucopyranoside, and the enzyme activity was measured by the colorimetric method (Ref. 20) using Alcian Blue 8 GX. Data are expressed as the mean  $\pm$  S.E., where  $n = 3$ . B, detection of hyaluronic acid-hydrolyzing proteins in sperm extracts. Proteins were separated by SDS-PAGE in the presence of hyaluronic acid under nonreducing conditions. The hyaluronic acid-hydrolyzing enzymes were visualized by staining the gels with Alcian Blue 8 GX and Coomassie Brilliant Blue R250. Note that a 52-kDa hyaluronic acid-hydrolyzing protein corresponding to PH-20 (Fig. 1D) is absent in the protein extracts of  $Ph20^{-/-}$  mouse sperm as indicated by an arrow. C, location of 55-kDa hyaluronic acid-hydrolyzing protein(s) in mouse sperm. Four protein fractions (AI, AR, SPA, and MPA) were prepared from cauda epididymal sperm of the  $Ph20^{+/+}$  and  $Ph20^{-/-}$  mice, separated by SDS-PAGE in the absence or presence (Hyase activity) of hyaluronic acid under nonreducing conditions, and analyzed by Western blotting using affinity-purified anti-mouse PH-20 antibody. As a control, affinity-purified antibody against an acrosomal proacrosin-binding protein, sp32, was also used.

consistent with the experimental data obtained by Western blot analysis (Fig. 1D).

To examine the location of a 55-kDa protein(s) and PH-20 exhibiting hyaluronidase activity in sperm, four protein fractions (AI, AR, SPA, and MPA) were prepared from epididymal sperm of  $Ph20^{+/+}$  and  $Ph20^{-/-}$  mice and analyzed by Western blotting using affinity-purified anti-mouse PH-20 antibody (Fig. 4C). Affinity-purified antibody against an acrosomal proacrosin-binding protein, sp32 (26, 27), was also used as a control. In the  $Ph20^{+/+}$  mouse, only the SPA fraction contained no PH-20, whereas the 55-kDa protein was abundantly present in the SPA fraction. In addition, PH-20 was absent in the AI, AR, and MPA fractions from the  $Ph20^{-/-}$  mouse. These data clearly demonstrate the presence of other hyaluronidase(s) besides PH-20 presumably within the acrosome of mouse sperm. It should be noted that a very small amount of the hyaluronidase activity resulting from the 55-kDa protein(s) is also found in AR fraction. This may be due to the presence of contaminating acrosome-intact sperm in the AR fraction, because only 80–90% of sperm were acrosome-reacted by calcium ionophore A23187 under the conditions employed in the present study. Indeed, acrosomal protein sp32 is slightly but significantly detectable in the AR fraction (Fig. 4C).

DISCUSSION

This study demonstrates both a partial contribution of mouse PH-20 toward the sperm penetration through the layer of cumulus cells (Figs. 2 and 3), and the presence of other hyaluronidase(s) besides PH-20 in mouse sperm (Fig. 4). PH-20 has long been thought to be the sole hyaluronidase involved in

sperm penetration through the cumulus cell layer, because other sperm hyaluronidases have not been characterized well. Our results indicate that a 55-kDa protein exhibiting hyaluronidase activity is abundantly released by calcium ionophore-induced acrosome reaction presumably from the acrosome (Fig. 4). If the acrosome reaction does not occur until acrosome-intact sperm reach the egg ZP, the 55-kDa hyaluronidase may be functional in the sperm/ZP interactions, including secondary sperm-ZP binding. It is also speculated that the motility may be the most important factor in the sperm penetration of the cumulus layer, if hyaluronidases other than PH-20 are absent on the sperm membrane. Thus, the other sperm hyaluronidases remain to be characterized.

Mice carrying either of two Robertsonian translocations on chromosome 6, Rb(6.16) and Rb(6.15), have been reported as showing a significant transmission ratio distortion in the progeny (transmission ratios of 3.6:1 and 2.4:1, respectively) (28–30), as found in the mice carrying different *t* alleles (31). The impaired fertility of Rb-bearing sperm seems to be the result of a decreased amount of hyaluronidase activity on the sperm membrane (32). The gene encoding sperm adhesion molecule 1, Spam1, identical to PH-20, is a candidate gene involved in the sperm dysfunction leading to transmission ratio distortion in the Rb(6.16) and Rb(6.15) mice (33). In the present study, the impaired ability of *Ph20*<sup>-/-</sup> mouse sperm to fertilize cumulus-intact eggs *in vitro* (Fig. 3) is apparently consistent with the dysfunction of Rb-bearing mouse sperm. However, *Ph20*<sup>-/-</sup> male mice produce a normal average litter size, in contrast with the Rb homozygous mice. These data imply that the dysfunction of Rb-bearing mouse sperm may not be ascribed solely to the reduced amount of sperm Spam1/PH-20.

The human and mouse genomes have been reported to possess six hyaluronidase-like genes, each three genes of which form a cluster on the chromosomes (34). In the mouse, three genes corresponding to the human *HYALP1*, *HYAL4*, and *PH-20/SPAM1* genes are clustered within the region of ~65 kbp on mouse chromosome 6 A2 (34). As far as we have examined, the mouse *HYALP1* and *PH-20/SPAM1* genes are both expressed exclusively in testicular tissues, whereas expression of the mouse *HYAL4* gene in the testis is barely detectable. We have also found the presence of an additional hyaluronidase-like gene (tentatively termed *HYAL5*) that is localized almost 100 kbp away from the *PH-20/SPAM1* gene on the mouse chromosome 6.<sup>2</sup> It has been demonstrated that multiple mutations occur in the *PH-20/SPAM1* gene of Rb(6.16) and Rb(6.15) mice because of recombination suppression near the Rb junctions (35), although no direct evidence has been provided that these mutations are responsible for the reduction in the hyaluronidase activity and gene expression. Even so, other point mutation(s) that affect the enzyme activity may occur in the *HYALP1* and *HYAL5* genes because of the localization adjacent to the *PH-20/SPAM1* gene on chromosome 6. Thus, additional experiments concerning possible mutations in the *HYALP1* and *HYAL5* genes would seem to be required. Moreover, it is important to ascertain whether these gene products are indeed present in mouse sperm.

The reduced rate of *Ph20*<sup>-/-</sup> mouse sperm in *in vitro* fertil-

ization with cumulus-intact eggs (Fig. 3) appears to be ascribable solely to the delayed penetration through the layer of cumulus cells. However, there is a possibility that an incomplete interaction between *Ph20*<sup>-/-</sup> sperm and egg ZP, because of the absence of PH-20, may result in the reduced fertilization rate. Our preliminary experiments indicate that no significant difference of ability to bind cumulus-free, ZP-intact eggs 30 min after insemination was observed among *Ph20*<sup>+/+</sup>, *Ph20*<sup>+/-</sup>, and *Ph20*<sup>-/-</sup> mouse sperm (numbers of sperm bound to ZP/egg = 8.8 ± 1.6, 11.3 ± 1.8, and 11.5 ± 2.2, respectively). These data appear to weaken the possible importance of PH-20 in the sperm/ZP interactions, although we have not yet examined the effects of mouse sperm lacking PH-20 on the secondary sperm-ZP binding using “live” acrosome-reacted sperm.

*Acknowledgment*—We thank Dr. P. Primakoff for the kind gift of recombinant mouse PH-20.

#### REFERENCES

- Laurent, T. C., and Fraser, J. R. E. (1992) *FASEB J.* **6**, 2397–2404
- Kreil, G. (1995) *Protein Sci.* **4**, 1666–1669
- Frost, G. I., Csoka, T., and Stern, R. (1996) *Trends Glycosci. Glycotechnol.* **8**, 419–434
- Yanagimachi, R. (1994) in *The Physiology of Reproduction* (Knobil, E., and Neill, J., eds) pp. 189–317, Raven Press, New York
- Myles, D. G., and Primakoff, P. (1997) *Biol. Reprod.* **56**, 320–327
- Wassarman, P. M. (1999) *Cell* **96**, 175–183
- Dandekar, P., Aggeler, J., and Talbot, P. (1992) *Hum. Reprod.* **7**, 391–398
- Primakoff, P., Hyatt, H., and Myles, D. G. (1985) *J. Cell Biol.* **101**, 2239–2244
- Phelps, B. M., Primakoff, P., Koppel, D. E., Low, M. G., and Myles, D. G. (1988) *Science* **240**, 1780–1782
- Gmachl, M., and Kreil, G. (1993) *Proc. Natl. Acad. Sci. U. S. A.* **90**, 3569–3573
- Gmachl, M., Sagan, S., Ketter, S., and Kreil, G. (1993) *FEBS Lett.* **336**, 545–548
- Thaler, C. D., and Cardullo, R. A. (1995) *Biochemistry* **34**, 7788–7795
- Cherr, G. N., Yudin, A. I., and Overstreet, J. W. (2001) *Matrix Biol.* **20**, 515–525
- Lin, Y., Mahan, K., Lathrop, W. F., Myles, D. G., and Primakoff, P. (1994) *J. Cell Biol.* **125**, 1157–1163
- Hunnicut, G. R., Primakoff, P., and Myles, D. G. (1996) *Biol. Reprod.* **55**, 80–86
- Baba, T., Azuma, S., Kashiwabara, S., and Toyoda, Y. (1994) *J. Biol. Chem.* **269**, 31845–31849
- Kashiwabara, S., Zhuang, T., Yamagata, K., Noguchi, J., Fukamizu, A., and Baba, T. (2000) *Dev. Biol.* **228**, 106–115
- Baba, T., Kashiwabara, S., Watanabe, K., Itoh, H., Michikawa, Y., Kimura, K., Takada, M., Fukamizu, A., and Arai, Y. (1989) *J. Biol. Chem.* **264**, 11920–11927
- Toyoda, Y., Yokoyama, M., and Hoshi, T. (1971) *Jpn. J. Anim. Reprod.* **16**, 147–151
- Pryce-Jones, R. H., and Lannigan, N. A. (1997) *J. Pharm. Pharmacol.* **31**, 92P
- Yamagata, K., Murayama, K., Okabe, M., Toshimori, K., Nakanishi, T., Kashiwabara, S., and Baba, T. (1998) *J. Biol. Chem.* **273**, 10470–10474
- Guntenhöner, M. W., Pogrel, M. A., and Stern, R. (1992) *Matrix* **12**, 388–396
- Yamagata, K., Murayama, K., Kohno, N., Kashiwabara, S., and Baba, T. (1998) *Zygote* **6**, 311–319
- Ho, Y., Wigglesworth, K., Eppig, J. J., Schultz, R. M. (1995) *Mol. Reprod. Dev.* **41**, 232–238
- Ohmura, K., Kohno, N., Kobayashi, Y., Yamagata, K., Sato, S., Kashiwabara, S., and Baba, T. (1999) *J. Biol. Chem.* **274**, 29426–29432
- Baba, T., Niida, Y., Michikawa, Y., Kashiwabara, S., Kodaira, K., Takenaka, M., Kohno, N., Gerton, G. L., and Arai, Y. (1994) *J. Biol. Chem.* **269**, 10133–10140
- Honda, A., Yamagata, K., Sugiura, S., Watanabe, K., and Baba, T. (2002) *J. Biol. Chem.* **277**, 16976–16984
- Aranha, I. P., and Martin-DeLeon, P. A. (1991) *Hum. Genet.* **87**, 278–284
- Chayko, C. A., and Martin-DeLeon, P. A. (1992) *Hum. Genet.* **90**, 79–85
- Aranha, I. P., and Martin-DeLeon, P. A. (1995) *Cytogenet. Cell Genet.* **69**, 253–259
- Silver, L. M. (1985) *Annu. Rev. Genet.* **19**, 179–208
- Zheng, Y., Deng, X., and Martin-DeLeon, P. A. (2001) *Biol. Reprod.* **64**, 1730–1738
- Zheng, Y., and Martin-DeLeon, P. A. (1999) *Mol. Reprod. Dev.* **54**, 8–16
- Csoka, A. B., Frost, G. I., and Stern, R. (2001) *Matrix Biol.* **20**, 499–508
- Zheng, Y., Deng, X., Zhao, Y., Zhang, H., and Martin-DeLeon, P. A. (2001) *Mamm. Genome* **12**, 822–829

<sup>2</sup> D. Baba and T. Baba, unpublished data.